IEEE Access
Multidisciplinary : Rapid Review : Open Access Journal

Received 13 December 2024, accepted 6 January 2025, date of publication 17 January 2025, date of current version 23 January 2025.

Digital Object Identifier 10.1109/ACCESS.2025.3531328

RESEARCH ARTICLE

A Testing Framework for Joint Communication and Sensing in Synthetic Aperture Radars

ALEX PICCIONI[1,2], (Member, IEEE), **ROBERTO ALESII**[1,2], (Member, IEEE), **FORTUNATO SANTUCCI**[1,2,3], (Senior Member, IEEE), AND **FABIO GRAZIOSI**[1,2], (Member, IEEE)
[1]DISIM Department, University of L'Aquila, 67100 L'Aquila, Italy
[2]National Inter-University Consortium for Telecommunications (CNIT), 43124 Parma, Italy
[3]EX-EMERGE Center of Excellence, University of L'Aquila, 67100 L'Aquila, Italy

Corresponding author: Alex Piccioni (alex.piccioni@univaq.it)

This work was supported in part by the Centre of EXcellence on Connected, Geo-Localized and Cybersecure Vehicles (EX-EMERGE), funded by the Italian Government (Inter-Ministerial Committee for Economic Planning (CIPE) under Resolution 70/2017); in part by the European Union under the Italian National Recovery and Resilience Plan (NRRP) of NextGenerationEU, through National Innovation Ecosystem under Grant ECS00000041–VITALITY–CUP E13C22001060006; and in part by the Telecommunications of the Future (Program "Research and Innovation on Future Telecommunications Systems and Networks (RESTART)"-PE00000001), Mission 4, Component 2, Investment 1.3, under Grant CUP D93C22000910001 and Grant CUP D43C22003080001.

Dedicated to the memory of Ascolino Bernardi, a bright colleague and dear friend

ABSTRACT Nowadays the modern progress in wireless communication technologies is motivating the mutual integration of heterogeneous services, in particular enabling resource and hardware-saving in platform deployment. In this perspective, Integrated Sensing and Communications (ISAC) is emerging as one of the most promising areas of research, especially for sensing technologies that are not originally designed for communication purposes, such as radar and Synthetic Aperture Radar (SAR). Current approaches leverage code modulation techniques through specific ground targets, which enable communication integration within SARs without requiring hardware modification. Besides, code transparency reduces the contribution of the target with low additive interference into the final SAR images. However, ISAC testing in real SAR systems poses numerous challenges. This paper introduces a novel testing framework that enables comprehensive evaluation of ISAC functionalities without the operational constraints of real-time tests. The framework provides flexibility across SAR platforms, operational parameters, and acquisition modes, ensuring practical, scalable, and cost-effective validation of communication embedding in SAR systems. To validate the proposed testing framework, real raw data from the ESA Sentinel-1 constellation have been employed to emulate ISAC target behaviour, demonstrating the effectiveness of the framework.

INDEX TERMS Integrated sensing and communication (ISAC), synthetic aperture radar (SAR), testing framework, backscattering communications, communication embedding.

I. INTRODUCTION

The rapid evolution of wireless communications technologies is driving significant changes in the way we use communication and sensing systems. Modern mobile networks, such as 5G and forthcoming 6G, exhibit impressive performance that enable a plethora of new services and applications. Simultaneously, sensing techniques are increasing popularity due to their ability to gather information about environments and phenomena, which is crucial for automation and situational awareness purposes. Remote sensing, in particular, has consolidated its role as an essential tool across various domains, including geology, meteorology, geophysics, military, humanitarian, and commercial applications.

The demands of emerging services are placing more challenging requirements on both communication and sensing technologies, including increased capacity, enhanced performance, resilience, reduced complexity, and energy

The associate editor coordinating the review of this manuscript and approving it for publication was Chuan Heng Foh.

efficiency. Communication and sensing systems have been traditionally developed independently, relying on different hardware technologies and separated spectral resources. However, recent efforts have focused on the integration of these technologies to improve efficiency, and boost overall system capabilities. These motivations [1], [2] paved the way for Integrated Sensing and Communication (ISAC), that has emerged as an attractive solution in both research activities and industrial development. ISAC is set to play a significant role in next-generation networks like 6G [3] by enhancing features such as location awareness and movement detection, thereby boosting efficiency and capacity. Following the International Telecommunication Union (ITU) report towards 2030 [4], communication systems can support sensing services at radio level through the concept of ''network as a sensor''. On the other side, communication can benefit from sensing techniques allowing the network to be cognitive about the surrounding area.

The growing interest in ISAC has resulted in increasing integration between communication and sensing services. For radar-based sensing applications and their derived technologies like Synthetic Aperture Radar (SAR), ISAC represents a near-term evolution due to the abundance of contexts wherein SARs are deployed and exploited. While a typical radar extracts information about a target transmitting a frequency-modulated signal (i.e., chirp), SAR leverages a large synthetic antenna aperture through the radar movement to perform daylight and weather independent acquisition of high-resolution images [5]. Various SAR acquisition techniques, such as stripmap, ScanSAR, spotlight, and TOPSAR, have been developed to improve critical aspects like image resolution and coverage area, where each technique employs different antenna and beam strategies to achieve specific trade-offs [5], [6], [7], [8].

Referring to the satellite scenario, SAR systems are often supported by ground targets for tasks such as radiometric calibration to correct functional parameters, geometric calibration to map the final pixels into specific locations, or high-level operations like geopositioning to monitor certain phenomena [9]. Corner Reflectors (CRs) are the most used targets due to their ability to backscatter the SAR signals with a Radar Cross-Section (RCS) higher than the surrounding environment, highlighting their position. In general, CRs are classified as passive (i.e., made by metal plate without power sources) or active, but recently a novel category of active CRs has been defined leveraging Software Defined Radio (SDR) technology, which enables the same features of classic CRs in addition to the advantages of digital signal processing [10].

Ground targets represent a valuable approach to integrate communication within a technology not originally aimed at this purpose. In fact, they provide a promising path to implement ISAC functionalities without requiring modifications in traditional SAR operations. Specific ground targets can be designed to reflect SAR signals while embedding communication through code modulation techniques [11], enabling joint sensing and communication tasks. Transparency represent a key aspect, allowing for the integration of embedded communication links without affecting the primary sensing capabilities of the SAR system. This integration provides additional information about targets and their environments, enhancing remote sensing capabilities without requiring dedicated sensors across the SAR coverage area. Moreover, the proposed setup facilitates an additive type of intermediate ground-satellite uplink, allowing for small-scale information exchange alongside the standard data transfer processes.

Nevertheless, verifying the ground target capabilities in real-world scenarios poses several challenges, such as the complexity of SAR acquisition, the strict timing requirements related to satellite orbits, and the regulatory constraints on signal emissions in licensed frequency bands. These challenges motivate the need for a flexible and scalable testing approach that can emulate real conditions without relying on real-time experiments. For this reason, this work presents a novel framework to test the joint sensing and communication functionality regardless the specific SAR technology. This framework can be adapted to various SAR platforms already on air, independently of operational parameters such as carrier frequency, bandwidth, acquisition mode, or SAR type (e.g., satellite, airborne). By utilizing real data acquired from SAR satellites, it allows for realistic emulation of targets and validation of joint sensing and communication functionality in realistic scenarios, ensuring continuity of traditional SAR operations without additive interference. The proposed framework plays a crucial role in validating the integration of communication in SAR systems, enabling the evaluation of the data transmission while ensuring transparency with respect to traditional SAR functionalities.

The rest of the paper is organized as follows: Section II provides an overview of the joint communication and sensing state of the art, followed by an accurate literature overview on radar and SAR communication integration. In Section III, we describe the functionality of the target used to embed the communication link in SAR technology and outline the system model considered in this work. Section IV introduces the proposed testing framework as well as the key assumptions. Section V presents and discusses the results obtained using real data obtained from on-air SAR satellites. Finally, Section VI provides concluding remarks on the activity and the description of future directions.

II. JOINT RADAR AND COMMUNICATION TECHNOLOGIES: TRENDS AND OPPORTUNITIES

ISAC has emerged as a key paradigm that includes a variety of systems, along with their set of applications and services. These includes mobile networks, indoor systems, Vehicle-To-Everything (V2X) communication, and radar-based remote sensing applications such as indoor localization and activity recognition [2], [12]. Following

Radar & Communication		SAR & Communication	ITU
Communication and Radar Spectrum Sharing (CRSS) Classification in primary and secondary services	[17]		
→ Radar-Communication Coexistence (RCC) Interference mitigation, non-cooperative	[17],[18]		Coexistence
→ Dual-Function Radar-Communication (DFRC) Cooperative, resources and information sharing	[22]-[24]	[34],[39],[40]	Cooperation
Radar-Communications or RadCom Single hardware for both services	[25],[26]		
Joint Communication and Radar (JCR) Communication-centric joint approach	[16],[27]	[41]	
Joint Radar and Communication (JRC) Radar-centric joint approach	[28],[29]	[35]-[38]	
Joint Communication And radar Sensing (JCAS) Ad hoc development, shared framework for waveform design	[30],[32],[33]	[40]	Co-Design

FIGURE 1. Summary of known radar & communication definitions, joint SAR&communication, and ITU-R classification [4]. Bibliographic references are mapped in the classification items.

ITU-R [4], joint communication and sensing systems are classified into three levels of integration:

- **Coexistence:** Communication and sensing operate as distinct technologies, each with physically separated hardware. They share the same spectral resources and employ interference mitigation techniques.
- **Cooperation:** Separate hardware for both technologies, exchanging information to minimize cross-interference and enhance the overall system performance.
- **Co-design:** Fully integrated systems that share information and utilize common frameworks for waveform design, offering native support for both functionalities.

Co-design represents the core level of ISAC paradigm, and different stages of ISAC development can be observed in practical implementations. In this sense, in autonomous vehicles and V2X connectivity, sensing techniques for detecting objects and pedestrians are integrated into low-latency communications, which helps prevent critical events and reduce traffic congestion [13]. Another emerging approach is the integration of sensing capabilities into cellular networks, enabling "sensing as a service" applications. In this case, the base stations are not used just for connectivity but also to sense the environment, providing valuable information such as the speed and position of multiple targets in urban environments with cars and pedestrians [14]. Remote sensing and geoscience represent another field where ISAC is emerging as a solution to integrate communication, with communication embedding as an interesting solution for the integration of low-throughput communications [11].

A. INTEGRATING RADAR AND COMMUNICATION: A STATE OF THE ART

Regarding radar technologies, ISAC is often employed to describe the integration from a generic point of view, and different names and acronyms have been defined in the literature. The integration of radar and communication systems has been extensively explored over the past decades [15], while today is well investigated by the research community and is still under analysis. Several definitions have been presented in literature, each one with different purposes and levels of combination [16]. A first classification is Communication and Radar Spectrum Sharing (CRSS) [17], which includes two type of integration: Radar-Communication Coexistence (RCC) and the Dual-Function Radar-Communication (DFRC).

In RCC, the focus is on the coexistence of radar and communication services that share the same resources (e.g., frequency, hardware, RF elements) while employing cross-technology interference mitigation techniques without losses in terms of performance [17], [18]. A common approach is the opportunistic spectrum access, where radar is considered the primary service and communication the secondary that exploits embedding techniques. As a result, RCC is generally classified as non-cooperative, while DFRC is considered cooperative, either where communication serves as the primary function facilitating sensing [19], or where radar serves as the primary function with communication embedded in radar waveforms [20]. DFRC systems can feature cooperation between single or multiple transceivers [21], as well as sidelobe management [22] and joint waveform design [23], [24].

Different names are used in literature to identify other joint approaches than CRSS. Radar-Communications or RadCom refers to systems that use a single hardware platform and a single waveform in automotive and Vehicle-to-Vehicle (V2V) scenarios [25], [26], often using spread spectrum and Orthogonal Frequency Division-Multiplexing (OFDM) techniques. Other common definitions are Joint Communication and Radar (JCR) [16], [27] and Joint Radar and Communication (JRC) [28], [29], which imply the same integration with

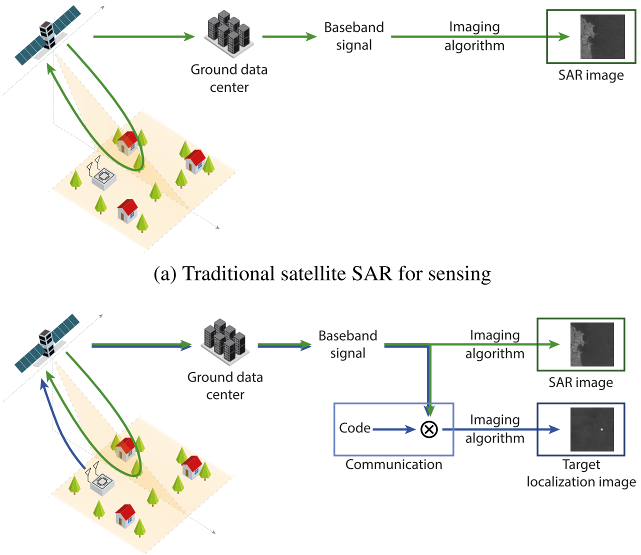

(a) Traditional satellite SAR for sensing

(b) Joint communication and sensing target in satellite SAR

FIGURE 2. **Schematic representations.**

a distinction between, respectively, communication-centric and radar-centric design. Joint Communication And radar Sensing (JCAS) [16], [30], [31] in general refers to a deeper level of integration classified as co-design [32], [33]. The primary and secondary classification falls apart in favor of a joint ad hoc system design capable of executing both services in a single or distributed device, which falls into the ISAC definition. In Fig.1 all the above definitions are summarized and referenced to the ITU-R integration classification listed in [4].

B. SAR-ENABLED COMMUNICATION AND SENSING

The integration of communication capabilities into SAR (Synthetic Aperture Radar) systems is still in its early stages. Unlike radar, which serves a wide array of applications, SAR is primarily used for remote sensing. One of the most common approaches involves embedding communication in SAR waveforms, as described in [34] with an uplink backscattering communication framework for target localization. OFDM, a key technique in modern wireless communication, has also demonstrated its effectiveness for SAR imaging [35], [36], [37], [38]. Additionally, watermarking represents another valid technique to develop a dual-function SAR and communication framework that relies on information embedding [39].

Reference [40] presents a novel approach for SAR communication embedding through time-frequency spectrum shaping, enabling the communication integration while keeping a high-performance imaging process. Differently, [41] describes a novel cellular-aided SAR system that leverages existing mobile communication base stations to enable bistatic SAR through Unmanned Aerial Vehicle (UAV) SAR receiver, thereby reversing the conventional approach by using communication signals for SAR imaging purposes.

III. ARCHITECTURE FOR INTEGRATING COMMUNICATION IN SAR SYSTEMS

Building on the foundational concepts and advancements discussed in the previous section, this section describes how the communication link is embedded in SAR technology and introduces the proposed system model.

A. COMMUNICATION EMBEDDING IN SAR

Joint communication and sensing functionality is implemented exploiting ad hoc ground targets, without necessitating updates or modifications to SAR satellites. This operation is performed through a code-based backscattering of the chirps emitted by the SAR satellite, leveraging the short time window during which the target of interest is illuminated to establish a low-capacity communication link. For this reason, target identification has been considered as a first service provided by the communication link, paving the way for more advanced transmissions in which codes serve as preamble matching. Additionally, each code bit is encoded to ensure transparency of the target in the final SAR image. This strategy aims to conceal the contribution of the target in the surrounding environment, as for steganography techniques where communication is hidden to facilitate secure exchange of information [42].

We assume that the proposed target is synchronized with the SAR, enabling communication when the target falls within the coverage area provided by the primary lobes of the SAR antenna. The target enforces a CR-based behaviour, with an amplitude control during the backscattering operation that enables the code-based modulation as for Binary Phase-Shift Keying (BPSK) technique to integrate the communication link. The target is aware of the time window in which is illuminated by the SAR, as well as its Pulse Repetition Interval (PRI), which is the time interval between the transmission of two consecutive chirps. We consider a relatively low duty cycle (i.e., below 10%), where the SAR transmits chirp signals and then collects all the echoes from the environment. The acquired baseband signals are then transferred to a ground processing center and made available for further processing. We assume that the acquired data result from a single acquisition, with a duration long enough to include the time window in which the ground target is highlighted by the SAR.

The traditional SAR image is obtained by processing the SAR data. In addition, the ISAC approach through communication embedding incorporates further results:

- **Integrated communication service**: Exploiting code demodulation and decoding, the embedded communication content is obtained. This integration includes services ranging from basic communication tasks like identification processes to more complex information exchange with higher data volumes [11].
- **Target localization**: It derives from traditional image processing of demodulated SAR data. Similar to Direct Sequence Spread Spectrum (DSSS) techniques, the

code-based approach reduces environmental contribution while highlighting the target, resulting in a second image suitable for geographic mapping and enabling target localization;
- **Target tracking**: This result is achieved by obtaining multiple target localization images from several SAR revisits, allowing to track the target trajectory.

The related additional processing stages are summarized in Fig.2, where the communication integration in SAR is represented in addition to the traditional SAR. The green path represents the logical steps to obtain the traditional SAR image from the data acquired by the satellite, while the blue path represents the steps to obtain the results described above.

B. SYSTEM MODEL

The following details the integration of a code-based communication link into a traditional SAR imaging system, focusing on satellite systems without loss of generality. Let us consider a generic ground target responsible for integrating communication into a SAR system operating in stripmap mode. It is worth noticing that the specific target backscatters a noise-like received signals that is superimposed on the usual ambient backscattering captured by SAR. This contribution must be obtained from the SAR signals by correlating it with a synthetic replica of the code used for communication.

The target embeds the communication link, where identification is considered as the first step to integrate communication within SARs, and is performed through code-matching. We assume a generic Pseudo-Noise (PN) code $\mathcal{C}_{PN} = c_{PN,1}, \ldots, c_{PN,L}$ for the communication integration, where $c_{PN,m} \in \{0, 1\}$ represents the m-th bit of the PN code, and L denotes the PN code length with $m = 1, \ldots, L$. The encoding operation ensures the code balance, which maintains the transparency of the target. Employing a two-level bipolar encoding technique, specifically Manchester encoding, each code bit $c_{PN,m}$ is mapped into a sequence of two symbols $[\pm 1, \mp 1]$. Thus, the sequence $\mathcal{C}_{PN}$ in mapped into the sequence $\mathcal{C} = \{c_1, \ldots c_{2L}\}$, with $c_i \in \{-1, +1\}$ and $i = 1, \ldots, 2L$.

The echoes received by the SAR satellite, corresponding to the position $(0, u)$ and the generic time instant t, can be expressed as [43]

$$s_{rx}(t, u) = \sum_n \sigma_n \, p\,(t - t_n) \tag{1}$$

where t is the temporal variable for the range direction, u is the spatial variable for the azimuth direction, with $u \in [-\frac{U}{2}, \frac{U}{2}]$ and U is the overall path length acquired by the SAR. It should be pointed out that the variable u identifies a specific SAR position where it collects chirp replicas backscattered by the environment. These replicas are linked to a specific PRI acquired by the satellite among the overall set of PRIs, thus correlating u with the PRIs. Moreover, the term

$$t_n = \frac{2}{c}\sqrt{x_n^2 + (y_n - u)^2} \tag{2}$$

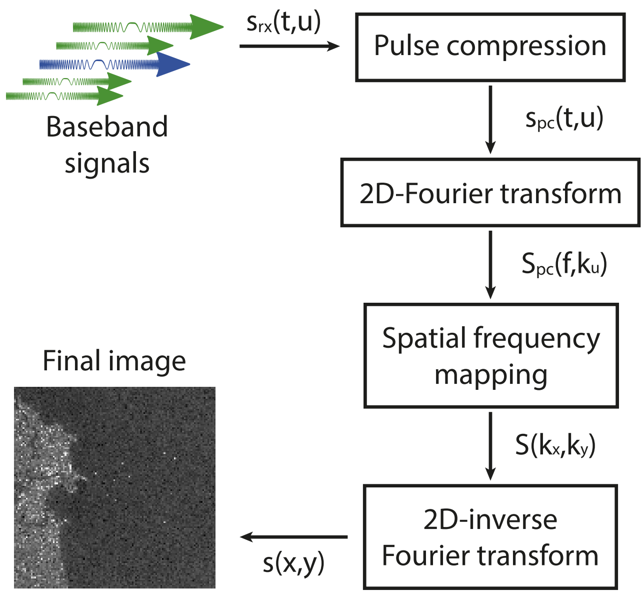

FIGURE 3. Summarized block diagram of the range migration algorithm.

represents the round-trip delay of the generic n-th environmental target, while (x_n, y_n) and σ_n are its relative coordinates compared to the satellite (x for the range and y for the azimuth) and reflectivity, respectively.

We assume (x_T, y_T) as the proposed target position and σ_T its reflectivity. Thus, we define $c_i \in \mathcal{C}$, with $i = 1, \ldots, 2L$, as the i-th symbol used to modulate the chirp received by the target at the time instant t. We define also N as the number of PRIs falling within the time interval during which the target is illuminated by the SAR. We assume $N > 2L$, such that the sequence $\mathcal{C}$ is cyclically repeated to cover the N PRIs. This cyclic repetition is considered specifically for identification tasks, while for enhanced communications the entire set of PRIs can be exploited to aggregate information contents. Integrating the target contribution in Eq. (1) we obtain

$$s_{rx}(t, u) = \sum_n \sigma_n \, p\,(t - t_n) + \sigma_T \, p\,(t - t_T)\, c_i \,\mathrm{rect}\left(\frac{u - i\Delta u}{\Delta u}\right) \tag{3}$$

where t_T is the round-trip delay of the target, *rect* is the rectangular function, and Δu is the spatial difference between two consecutive SAR positions (i.e. PRIs), which is expressed as the product between the PRI and the SAR speed. The second term of Eq. (3) represents the contribution due to the target, which is similar to ambient targets in addition to the contribution of the embedded communication. The generic symbol c_i is opportunely shifted in the azimuth direction to align with respect to the specific SAR PRI.

Referring to [43], we assume the range migration algorithm [44], summarized in Fig.3, to generate the final image from the baseband SAR signals. Performing Pulse

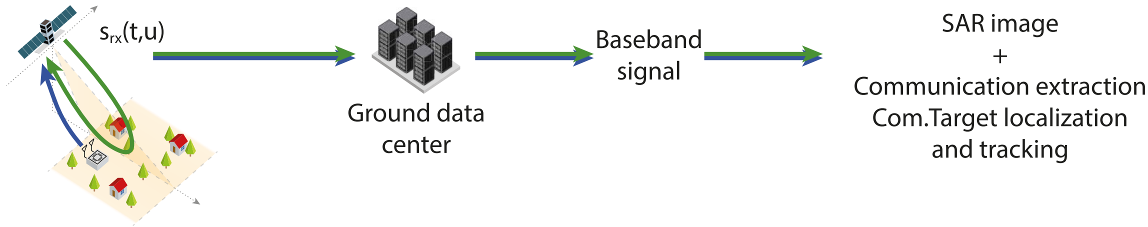

(a) On-site testing scenario

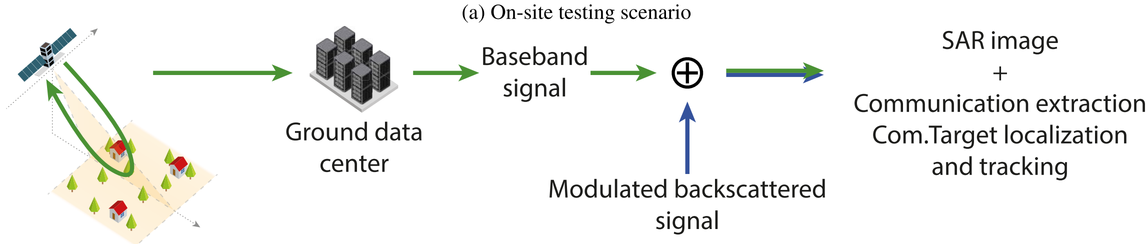

(b) Proposed testing framework

FIGURE 4. Simplified representation from Fig.2 with a comparison between on-site testing and the proposed testing framework with synthetic modulated backscattering signals.

Compression (PC) on Eq. (3) and after some reorganizations, we obtain

$$\begin{aligned} s_{pc}(t,u) &= s_{rx}(t) \otimes p^*(-t) = \mathcal{F}^{-1}\left\{|P(f)|^2\right\} \\ &\otimes \left[\sum_n \sigma_n\, \delta(t-t_n) + \sigma_T\, \delta(t-t_T)\, c_i \,\mathrm{rect}\left(\frac{u-i\Delta u}{\Delta u}\right)\right] \end{aligned} \tag{4}$$

where δ is the Dirac delta function and $\otimes$ is the convolution product. The 2D Fourier transform is exploited to process both the range and azimuth dimensions. Performing the Fourier transform on range dimension, we obtain

$$\begin{aligned} S_{pc}(f,u) = |P(f)|^2 \cdot \Bigg[\sum_n \sigma_n\, e^{-j2\pi f t_n} \\ + \sigma_T\, e^{-j2\pi f t_T}\, c_i \,\mathrm{rect}\left(\frac{u-i\,\Delta u}{\Delta u}\right)\Bigg] \end{aligned} \tag{5}$$

For the azimuth dimension, we move from spatial domain u to spatial frequency k_u. Replacing the round-trip delays as defined in Eq. (2) and applying the Fourier transform, Eq. (5) turns into

$$\begin{aligned} &S_{pc}(f,k_u) \\ &= |P(f)|^2 \cdot \Bigg[\sum_n \sigma_n\, e^{-j\left(x_n\sqrt{4k^2-k_u^2}+y_n k_u\right)} + \\ &+ \sigma_T\, e^{-j\left(x_T\sqrt{4k^2-k_u^2}+y_T k_u\right)} \cdot c_i\, \Delta u\, \mathrm{sinc}(k_u \Delta u) e^{-jk_u i\,\Delta u)}\Bigg] \end{aligned} \tag{6}$$

where $k = \frac{2\pi f}{c}$ is the wavenumber and *sinc* the normalized sinc function.

Applying SAR spatial frequency mapping [43], also known as the Stolt interpolation method

$$\begin{cases} k_x(f,k_u) = \sqrt{4k^2 - k_u^2} \\ k_y(f,k_u) = k_u \end{cases} \tag{7}$$

the frequency f and the spatial frequency k_u variables are transformed into spatial frequencies (k_x, k_y). Defining $S(k_x, k_y)$ as the resulting Eq. (6) after the Stolt interpolation, we obtain

$$\begin{aligned} &S(k_x,k_y) \\ &= \left|P(k_x,k_y)\right|^2 \cdot \Bigg[\sum_n \sigma_n\, e^{-j\left(x_n k_y + y_n k_y\right)} + \\ &+ \sigma_T\, e^{-j\left(x_n k_y + y_n k_y\right)} c_i\, \Delta u\, \mathrm{sinc}(k_u \Delta u) e^{-jk_u\, i \Delta u}\Bigg] \end{aligned} \tag{8}$$

Finally, performing the 2D Inverse Fourier transform and simplifying the result, Eq. (8) becomes

$$\begin{aligned} s(x,y) = A(x,y) \cdot \Bigg[\sum_n \sigma_n\, \delta\,(x-x_n, y-y_n) + \\ + \sigma_T \delta\,(x-x_T)\, c_i \,\mathrm{rect}\left(\frac{y-y_T - i\Delta u}{\Delta u}\right)\Bigg] \end{aligned} \tag{9}$$

where $A(x,y) = \mathcal{F}_{2D}^{-1}\left\{\left|P(k_x,k_y)\right|^2\right\}$ is the amplitude function, which depends on the specific transmitted signal $p(t)$. $s(x,y)$ represents the contribution of all the targets illuminated by the SAR at the position $(0,u)$ and time instant t.

The component related to the communication target is composed of two factors. The first depends on target position, likewise environmental targets, while the second results from communication embedding. Considering the overall SAR acquisition, the final image is derived by summing each $s(x,y)$ obtained in every position $u \in [-\frac{U}{2}, \frac{U}{2}]$. The ground target contribution resulting from communication embedding corresponds to a shifted sum in the azimuth direction, whose amplitude is influenced by the sequence $\mathcal{C}$. The transparency is ensured considering two consecutive acquisitions, where the communication target contribution in two consecutive SAR acquisitions made at positions $(0, u)$ and $(0, u + \Delta u)$ can be expressed as

$$\sigma_T \delta\left(x - x_T\right) \cdot \left[c_i\, rect\left(\frac{y - y_T - i\Delta u}{\Delta u}\right) + c_{i+1}\, \text{rect}\left(\frac{y - y_T - (i+1)\,\Delta u}{\Delta u}\right)\right] \tag{10}$$

which is equal to 0 since $c_{i+1} = -c_i$, while the additive Δu of the second term in Eq. (10) compensates for the shifted SAR position $(0, u + \Delta u)$.

IV. TESTING FRAMEWORK

A. FRAMEWORK MOTIVATION

The motivations behind the proposed testing framework are driven by several key factors. Traditional testing methods are constrained by regulatory restrictions (i.e., signal emissions in licensed frequency bands), practical difficulties associated with real-world tests, strict timing synchronization requirements, the dependency on convenient environmental conditions, and high costs and logistical complexities of deploying and managing real-time experiments. To address these issues, we propose an alternative approach based on a novel testing framework that leverages real SAR data to validate the joint sensing and communication target.

This approach allows for realistic and detailed emulation of proposed targets and their interactions, offering a flexible, cost-effective, and practical solution to validate joint sensing and communication functionalities with high fidelity and without requiring real-time signal transmission or modifications to the SAR systems themselves. The framework remains independent of the specific type of SAR system, whether airborne or satellite-based, as well as the specific signal used by the SAR. Moreover, it enables performance evaluation of joint communication and sensing tasks without operational constraints imposed by on-site and real-time testing. Additionally, it facilitates the evaluation in different locations based on the SAR acquisitions from different geographical areas.

This independence is achieved by exploiting a synthetic replica of the specific SAR signal, enabling the emulation of target behavior. Consequently, the proposed framework provides significant flexibility in adapting to heterogeneous SAR platforms and signals, enabling realistic and detailed emulation of proposed targets and their interactions with further SAR processing operations. The framework supports the emulation of different target scenarios, including varying signal strengths and target positions relative to the SAR's field of view. This flexibility is crucial for comprehensive testing and validation of ISAC concepts under diverse conditions, ensuring robustness and reliability of the proposed solutions.

Despite the significant flexibility in adapting to various SAR systems with different characteristics, several limitations must be considered. A major limitation derives from the dependency on SAR data provided by specific SAR platforms. Although the framework is designed to be versatile across different SAR systems, the accessibility of these systems is not always guaranteed, as many SAR platforms are not open. In some cases, special agreements may be required to access the raw data collected by the satellites. Additionally, managing the diverse calibration techniques employed by different SAR systems adds another layer of complexity. Each SAR system may use unique calibration parameters and techniques, making it difficult to ensure consistency and accuracy across multiple datasets, thus impacting the reliability of the emulated scenarios in the framework. Despite this, the framework remains versatile and adaptable to a wide range of SAR systems.

B. DETECTION OF COMMUNICATION COMPONENT

In the proposed framework, the detection of the communication component is performed to obtain the results described in section III-A. This approach ensures that the overall process, i.e., code matching and the subsequent localization image, is accurately tested in emulated conditions similar to traditional SAR data processing, providing a comprehensive understanding of system performance. We consider the raw data acquired by the satellite as In-Phase and Quadrature (I/Q) format. As described in the previous section, the resulting I/Q raw data are then processed using imaging algorithms, such as the aforementioned range migration algorithm, to generate the traditional SAR image. To extract the information embedded by the communication ground target, demodulation is applied according to the specific family of PN codes adopted.

Assuming $\boldsymbol{\mathcal{C}} = \mathcal{C}_1, \ldots, \mathcal{C}_P$ as the set of P PN codes resulting from the encoding operation, the detection of the embedded information involves the correlation across P parallel lines between the raw data and each code $\mathcal{C}_p$, for $p = 1, \ldots, P$. The communication component is obtained with two operations, the synchronization with the targets, and the code detection from set $\boldsymbol{\mathcal{C}}$. To synchronize with the target and correctly detect the communication component, the generic p-th line performs a 2D cross-correlation between the raw data and code $\mathcal{C}_p$ to highlight the code contribution. Calling back N as the number of PRI in which the target is illuminated, the 2D cross-correlation is executed considering a window w of length N containing the code $\mathcal{C}_p$ opportunely repeated to fit the window length. Then, code detection is performed by selecting the line $\bar{p}$ with the highest cross-correlation. Once synchronization with the target is achieved and communication code $\mathcal{C}_{\bar{p}}$ is detected, the raw data are opportunely demodulated under the window w by multiplying each PRI with the corresponding code bit of the window containing the code $\mathcal{C}_{\bar{p}}$. The demodulated raw data are then processed following traditional SAR imaging algorithms to generate the localization images.

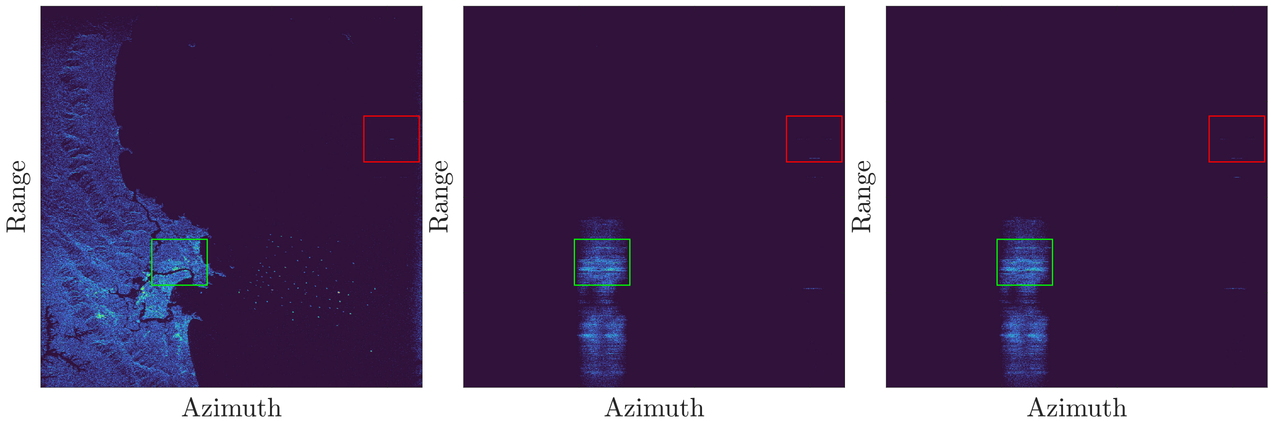

(a) SAR image (b) Localization image with code C_1 (c) Localization image with code C_2

FIGURE 5. Images of São Paulo, Brazil, obtained from ESA Sentinel-1 baseband signals processed with range migration algorithm for Position 1 (in red) and Position 2 (in green). The localization images are processed only in the area of interest after the detection of communication component.

C. FRAMEWORK ASSUMPTIONS

Assuming known specifications about the SAR system and the transmitted chirp, our framework relies on locally-generated chirp copies to emulate target backscattering. We also assume that the local copies are time-aligned, for instance by adopting GNSS signals while accounting for the satellite-to-ground path delay, ensuring realistic emulation of joint sensing and communication functionalities. Furthermore, it allows to replicate real testing conditions, as depicted in Fig. 4 where both the real test (Fig. 4a) and the testing framework (Fig. 4b) are illustrated.

A local set of the chirp replicas in I/Q components is generated, incorporating both the proposed target and its communication link through backscattering emulation and code modulation, respectively. Moreover, these replicas take into account the time instant within each PRI and the set of PRIs during which the proposed target is illuminated by the SAR, allowing for the emulation of a specific position within the final image. For this purpose, we consider two assumptions:

- The amplitude of each local chirp is lower at the beginning and end of the set, and reaches its maximum in the middle, emulating the maximum backscatter amplitude with the maximum antenna gain and the minimum SAR-to-target distance. Vice versa, reduced antenna gain and greater distances are emulated at the edges of the PRI set.
- The temporal position of the local chirp within each PRI varies throughout the set, emulating the increasing distance between the SAR and the target at the beginning and end of the set, with the distance being minimized in the middle.

V. EMULATION RESULTS

The proposed testing framework has been evaluated using real raw data from Sentinel-1 constellation of the European Space Agency (ESA) available through the ESA Copernicus platform [45]. These data are open and accessible, providing a robust basis for validating the framework across wide variety of heterogeneous applications. Sentinel-1 constellation provides global coverage, ensuring data availability across different geographical locations with different acquisition modes. The data acquired by Sentinel-1 are available in various formats, ranging from compressed raw data (Level-0) to pre-processed products (Level-1 and Level-2), which include different levels of analysis and processing. Information about Sentinel-1 constellation and the raw data considered for this work are reported in Table 1, while further information can be found at [46].

TABLE 1. Sentinel-1 parameters and specifications.

Parameter	Value
Satellite altitude	693 km
Acquisition modes	Stripmap
Spatial resolution	5x5 m
Carrier frequency	5.405 GHz
Bandwidth	$\sim$ 42 MHz
PRF	$\sim$ 1.69 kHz
Chirp duration	$\sim$ 51 μs
Data compression	FDBAQ
SAR coverage time interval	$\sim$ 0.49 s
SAR coverage PRIs	825
Revisit period	12 days

We considered the raw data acquired in the city of São Paulo, Brazil to evaluate the testing framework. This choice is due to the high contrast between the land, which is abundant in natural and man-made reflectors, and the Atlantic Ocean, which exhibits low reflectivity at C-band frequencies. Using Sentinel-1 stripmap parameters—among which its PRI, antenna azimuth angles and beam width, satellite speed, and incident angle—a set of $N = 825$ PRIs has been considered to emulate the time interval in which the target is illuminated.

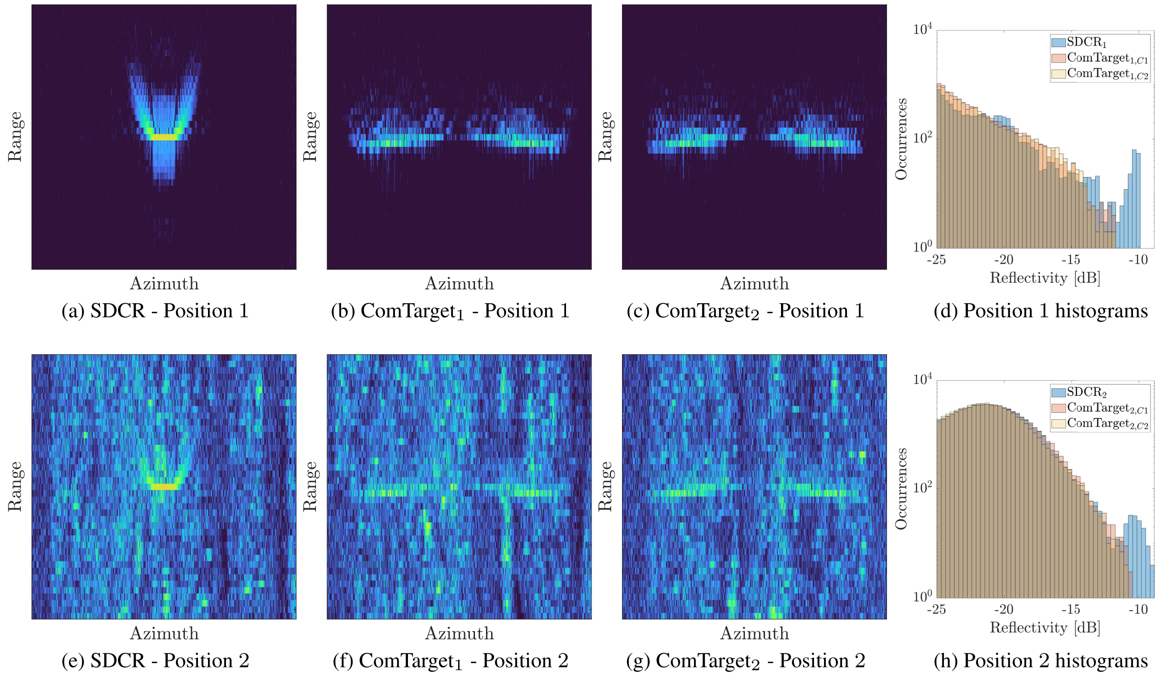

FIGURE 6. Zoom of SDCR, ComTarget$_1$, and ComTarget$_2$ in the SAR image with the histogram comparison in Position 1 and Position 2.

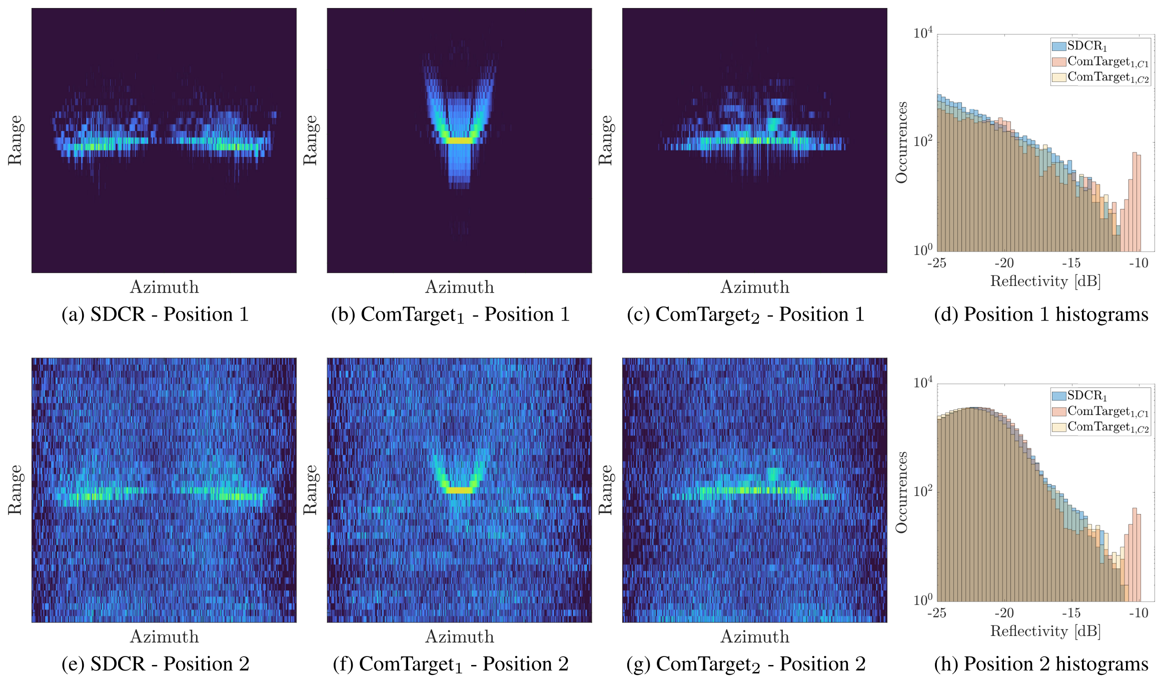

FIGURE 7. Zoom of SDCR, ComTarget$_1$, and ComTarget$_2$ in the Localization image (C_1) with the histogram comparison in Position 1 and Position 2.

It must be noticed that this value is consistent with the correlation peaks analysis of the raw data after the pulse compression for a generic environmental target. The raw data from Sentinel-1 have been decompressed [47] and processed using the range migration algorithm to generate the final images from the I/Q components [44], which are shown in Fig. 5. From this point onward, we refer to the final image obtained from the raw data as *SAR image*. Instead, we refer to *Localization image* (C_1) and *Localization image* (C_2) for the images obtained from the demodulated raw data when correlating with code C_1 and C_2, respectively.

The communication integration has been performed as an identification task. In this perspective, we refer to low cross-correlation codes with high auto-correlation

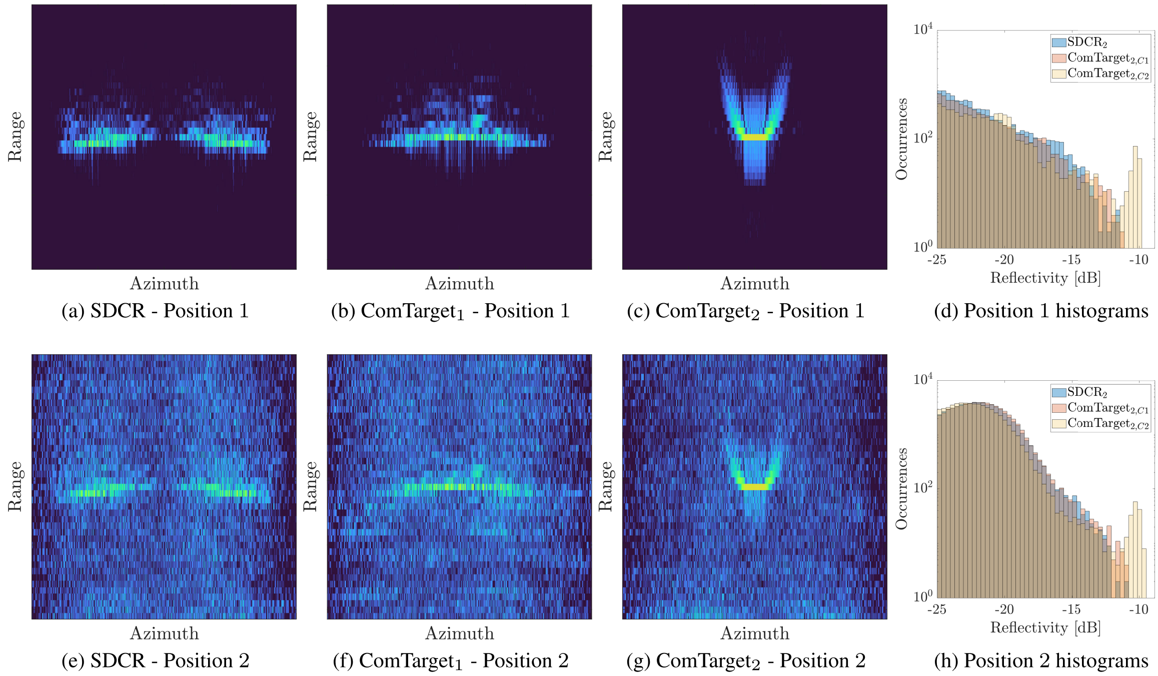

FIGURE 8. Zoom of SDCR, ComTarget$_1$, and ComTarget$_2$ in the Localization image (C_2) with the histogram comparison in Position 1 and Position 2.

peaks to effectively highlight the target contribution during demodulation. Two communication targets (*ComTarget*$_1$ and *ComTarget*$_2$) have been emulated implementing two different Kasami codes: $C_{PN,1}$ with length $L_{PN,1} = 255$ and $C_{PN,2}$ with length $L_{PN,2} = 63$. The codes have been opportunely encoded using Manchester encoding, resulting in sequences C_1 and C_2 with lengths $L_1 = 510$ and $L_2 = 126$, respectively. Additionally, an SDCR target [10] has been emulated in the proximity of ComTarget$_1$ and ComTarget$_2$ to evaluate traditional SAR operation while evaluating joint sensing and communication functionality. It should be mentioned that the use of the framework with the possibility of operating in the same geographical area of interest requires the acquisition of the signal received by ground targets. In any case, the framework enables the study of the sensing and communication integration problem without constraints on the choice of the technology used for communication integration. The different target types, corner reflector (i.e., SDCR) and communication target, have been considered in two different area reflecting different conditions: Position 1 (Fig. 5, marked in red), corresponding to a water area with very low RCS, and Position 2 (Fig. 5, marked in green), a land area with higher peak and average RCS. The local replicas of targets and SDCRs have been appropriately scaled according to the characteristics of a generic environmental target in the water area, as observed in the raw data. The raw data have been demodulated by correlating with codes C_1 and C_2 to generate two localization images (Fig. 5b and Fig. 5c) alongside the SAR image shown in Fig. 5a.

Fig. 6 exhibits the results for Position 1 and 2, comparing SDCRs (Fig. 6a and Fig. 6e) with ComTarget1 integrating code C_1 backscattering (Figs. 6b and 6f)and ComTarget2 integrating code C_2 backscattering (Fig. 6c and Fig. 6g). Position 1 highlights the effectiveness of the joint communication and sensing functionality for both codes while ensuring transparency, with code C_1 that slightly outperforms code C_2. However, each target presents a residual contribution spread in the azimuth direction resulting from the sum of the shifted replicas described by the second term of Eq. (9), which depends on the sequences C_1 and C_2. Fig. 6d and Fig. 6h present histograms of the zoomed images to compare the reflectivity of targets and SDCR at Position 1 and Position 2. The histograms indicate reduced contributions from ComTarget$_1$ and ComTarget$_2$ due to the code modulation, resulting in a greater number of pixels with low reflectivity compared to the SDCR.

Fig. 7 and Fig. 8 show zoomed images of the emulated targets and SDCRs for the demodulated raw data with codes C_1 and C_2 presented in Figs. 5b and 5c, respectively. The SDCRs (Figs.7a, 7e, 8a, and 8e) exhibit residual contributions spread in the azimuth direction, while Figs. 7b and 7f highlight the contributions of the proposed targets for code C_1, and Fig. 8b and Fig. 8f for code C_2, enabling the localization of the targets. This results from the code matching, which allows the detection of the targets in the final images, thereby enabling precise localization. This distinction in localization accuracy between the two codes underlines the effectiveness of the selected modulation scheme and provides valuable insights for optimizing target detection in similar environments. However, cross-correlation between codes can be observed in Figs. 7c, 7g, 8b, and 8f, corresponding to the demodulation of unmatched codes. The reduced contribution of the SDCR is also highlighted in the histograms (Figs. 7d, 7h, 8d, and 8h), where the zoomed SDCR images exhibit lower reflectivity

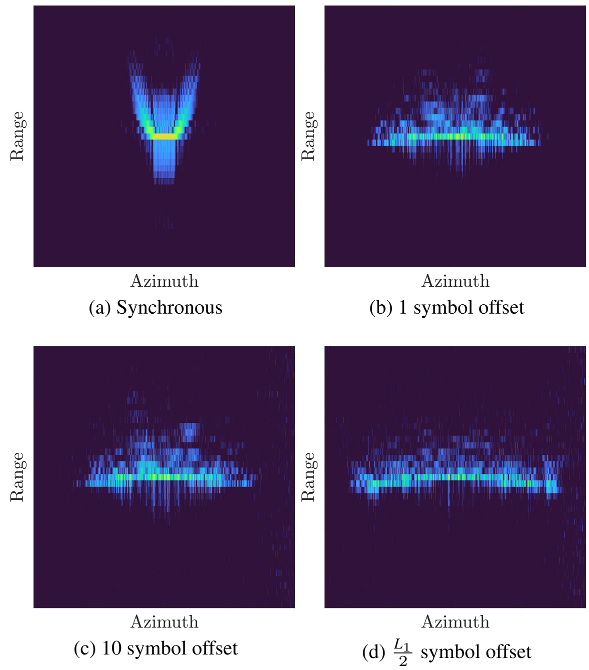

FIGURE 9. C_1 code synchronization for $ComTarget_1$ in Position 1.

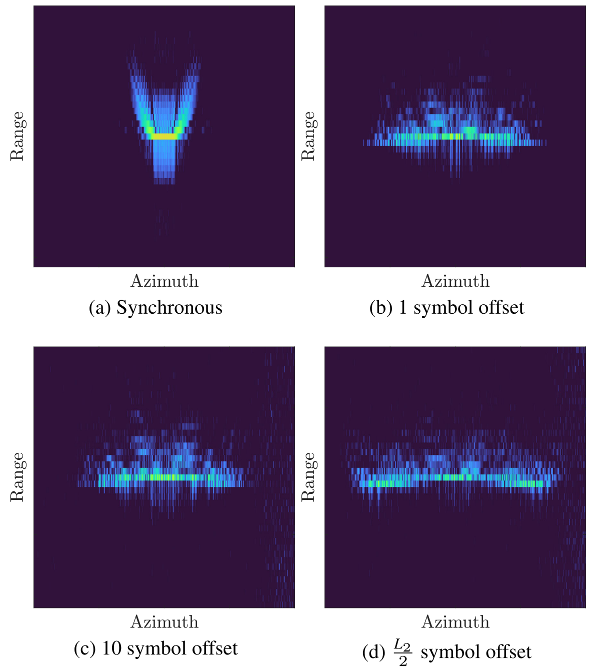

FIGURE 10. C_2 code synchronization for $ComTarget_2$ in Position 1.

compared to the targets. Moreover, the comparison between Fig. 6h with Figs. 7h and 8h shows the effect of demodulation process, with an higher number of pixels with low reflectivity for the demodulated images, especially in Position 2.

Finally, Figs. 9 and 10 illustrate the effects of inaccurate code synchronization between the raw data during demodulation step for $ComTarget_1$ and $ComTarget_2$, respectively, evaluated in Position 1. It can be noticed that wrong synchronization of 1 symbol leads to a target contribution spread in the azimuth direction, whose effect is due to the autocorrelation properties of the code.

VI. CONCLUSION

With the rapid advancements in wireless communications networks, the convergence of sensing and communication services is becoming popular for many purposes and applications, including radar and SAR technologies. Exploiting ground targets, ISAC concepts can be integrated into established SAR systems, thus introducing a communication link into sensing-oriented technology. This paper has demonstrated its potential through a novel testing framework based on target emulation that relies on real raw data acquired from the ESA Sentinel-1 satellite in stripmap mode. The framework validates the transparent ISAC approach while ensuring the continuity of SAR operations without interference. Further investigations will look at several directions, focusing on the minimization of the residuals due to transparency, the selection of optimal codes to enhance the performance, and integrating impedance-controlled devices (i.e., CRs) to facilitate communication integration. Moreover, future works will focus on communication performance, aiming to characterize the communication link also exploiting real environment tests.

ACKNOWLEDGMENT

Fortunato Santucci would like to acknowledge Ascolino Bernardi for his distinguished career with Thales Alenia Space: Ascolino, who astonishingly passed away a few months ago, played a pioneering role in the design of cutting-edge digital integrated circuits for several demanding satellite payloads.

REFERENCES

[1] A. Liu, Z. Huang, M. Li, Y. Wan, W. Li, T. X. Han, C. Liu, R. Du, D. K. P. Tan, J. Lu, Y. Shen, F. Colone, and K. Chetty, "A survey on fundamental limits of integrated sensing and communication," *IEEE Commun. Surveys Tuts.*, vol. 24, no. 2, pp. 994–1034, 2nd Quart., 2022.

[2] B. Paul, A. R. Chiriyath, and D. W. Bliss, "Survey of RF communications and sensing convergence research," *IEEE Access*, vol. 5, pp. 252–270, 2017.

[3] *The 6G Architecture Landscape*, 5G Infrastruct. Public Private Partnership (5G PPP), Eur. Union, Feb. 2023.

[4] ITU-R, *Future Technology Trends of Terrestrial International Mobile Telecommunications Systems Towards 2030 and Beyond*, document ITU-R M.2516-0, Nov. 2022.

[5] A. Moreira, P. Prats-Iraola, M. Younis, G. Krieger, I. Hajnsek, and K. P. Papathanassiou, "A tutorial on synthetic aperture radar," *IEEE Geosci. Remote Sens. Mag.*, vol. 1, no. 1, pp. 6–43, Mar. 2013.

[6] R. Moore, J. Claassen, and Y. H. Lin, "Scanning spaceborne synthetic aperture radar with integrated radiometer," *IEEE Trans. Aerosp. Electron. Syst.*, vols. AES-17, no. 3, pp. 410–421, May 1981.

[7] M. Eineder, N. Adam, R. Bamler, N. Yague-Martinez, and H. Breit, "Spaceborne spotlight SAR interferometry with TerraSAR-X," *IEEE Trans. Geosci. Remote Sens.*, vol. 47, no. 5, pp. 1524–1535, May 2009.

[8] F. De Zan and A. Monti Guarnieri, "TOPSAR: Terrain observation by progressive scans," *IEEE Trans. Geosci. Remote Sens.*, vol. 44, no. 9, pp. 2352–2360, Sep. 2006.

[9] M. Jauvin, Y. Yan, E. Trouvé, B. Fruneau, M. Gay, and B. Girard, "Integration of corner reflectors for the monitoring of mountain glacier areas with Sentinel-1 time series," *Remote Sens.*, vol. 11, no. 8, p. 988, Apr. 2019.

[10] A. Piccioni, R. Alesii, F. Santucci, and F. Graziosi, "Software-defined corner reflector for satellite SAR systems," in *Proc. IEEE Aerosp. Conf. (AERO)*, Mar. 2022, pp. 1–7.
[11] A. Piccioni, R. Alesii, F. Santucci, and F. Graziosi, "SDR-based ground target for identification and tracking through satellite SAR systems," in *Proc. IEEE Aerosp. Conf.*, Mar. 2021, pp. 1–10.
[12] F. Liu, Y. Cui, C. Masouros, J. Xu, T. X. Han, Y. C. Eldar, and S. Buzzi, "Integrated sensing and communications: Toward dual-functional wireless networks for 6G and beyond," *IEEE J. Sel. Areas Commun.*, vol. 40, no. 6, pp. 1728–1767, Jun. 2022.
[13] X. Cheng, D. Duan, S. Gao, and L. Yang, "Integrated sensing and communications (ISAC) for vehicular communication networks (VCN)," *IEEE Internet Things J.*, vol. 9, no. 23, pp. 23441–23451, Dec. 2022.
[14] L. Pucci, E. Paolini, and A. Giorgetti, "System-level analysis of joint sensing and communication based on 5G new radio," *IEEE J. Sel. Areas Commun.*, vol. 40, no. 7, pp. 2043–2055, Jul. 2022.
[15] R. M. Mealey, "A method for calculating error probabilities in a radar communication system," *IEEE Trans. Space Electron. Telemetry*, vol. SET-9, no. 2, pp. 37–42, Jun. 1963.
[16] J. A. Zhang, F. Liu, C. Masouros, R. W. Heath, Z. Feng, L. Zheng, and A. Petropulu, "An overview of signal processing techniques for joint communication and radar sensing," *IEEE J. Sel. Topics Signal Process.*, vol. 15, no. 6, pp. 1295–1315, Nov. 2021.
[17] F. Liu, C. Masouros, A. P. Petropulu, H. Griffiths, and L. Hanzo, "Joint radar and communication design: Applications, state-of-the-art, and the road ahead," *IEEE Trans. Commun.*, vol. 68, no. 6, pp. 3834–3862, Jun. 2020.
[18] L. Zheng, M. Lops, Y. C. Eldar, and X. Wang, "Radar and communication coexistence: An overview: A review of recent methods," *IEEE Signal Process. Mag.*, vol. 36, no. 5, pp. 85–99, Sep. 2019.
[19] A. Gameiro, D. Castanheira, J. Sanson, and P. P. Monteiro, "Research challenges, trends and applications for future joint radar communications systems," *Wireless Pers. Commun.*, vol. 100, no. 1, pp. 81–96, May 2018, doi: 10.1007/s11277-018-5614-8.
[20] S. D. Blunt, P. Yatham, and J. Stiles, "Intrapulse radar-embedded communications," *IEEE Trans. Aerosp. Electron. Syst.*, vol. 46, no. 3, pp. 1185–1200, Jul. 2010.
[21] F. Liu, A. Garcia-Rodriguez, C. Masouros, and G. Geraci, "Interfering channel estimation in radar-cellular coexistence: How much information do we need?" *IEEE Trans. Wireless Commun.*, vol. 18, no. 9, pp. 4238–4253, Sep. 2019.
[22] A. Hassanien, M. G. Amin, Y. D. Zhang, and F. Ahmad, "Dual-function radar-communications: Information embedding using sidelobe control and waveform diversity," *IEEE Trans. Signal Process.*, vol. 64, no. 8, pp. 2168–2181, Apr. 2016.
[23] F. Liu, L. Zhou, C. Masouros, A. Li, W. Luo, and A. Petropulu, "Toward dual-functional radar-communication systems: Optimal waveform design," *IEEE Trans. Signal Process.*, vol. 66, no. 16, pp. 4264–4279, Aug. 2018.
[24] D. Ma, N. Shlezinger, T. Huang, Y. Liu, and Y. C. Eldar, "Joint radar-communication strategies for autonomous vehicles: Combining two key automotive technologies," *IEEE Signal Process. Mag.*, vol. 37, no. 4, pp. 85–97, Jul. 2020.
[25] C. Sturm and W. Wiesbeck, "Waveform design and signal processing aspects for fusion of wireless communications and radar sensing," *Proc. IEEE*, vol. 99, no. 7, pp. 1236–1259, Jul. 2011.
[26] Y. Huang, S. Hu, S. Ma, Z. Liu, and M. Xiao, "Designing low-PAPR waveform for OFDM-based RadCom systems," *IEEE Trans. Wireless Commun.*, vol. 21, no. 9, pp. 6979–6993, Sep. 2022.
[27] P. Kumari, J. Choi, N. González-Prelcic, and R. W. Heath, "IEEE 802.11ad-based radar: An approach to joint vehicular communication-radar system," *IEEE Trans. Veh. Technol.*, vol. 67, no. 4, pp. 3012–3027, Apr. 2018.
[28] N. C. Luong, X. Lu, D. T. Hoang, D. Niyato, and D. I. Kim, "Radio resource management in joint radar and communication: A comprehensive survey," *IEEE Commun. Surveys Tuts.*, vol. 23, no. 2, pp. 780–814, 2nd Quart., 2021.
[29] Z. Feng, Z. Fang, Z. Wei, X. Chen, Z. Quan, and D. Ji, "Joint radar and communication: A survey," *China Commun.*, vol. 17, no. 1, pp. 1–27, Jan. 2020.
[30] M. Nemati, Y. H. Kim, and J. Choi, "Toward joint radar, communication, computation, localization, and sensing in IoT," *IEEE Access*, vol. 10, pp. 11772–11788, 2022.
[31] J. A. Zhang, Md. L. Rahman, K. Wu, X. Huang, Y. J. Guo, S. Chen, and J. Yuan, "Enabling joint communication and radar sensing in mobile networks—A survey," *IEEE Commun. Surveys Tuts.*, vol. 24, no. 1, pp. 306–345, 1st Quart., 2022.
[32] Md. L. Rahman, J. A. Zhang, X. Huang, Y. J. Guo, and R. W. Heath, "Framework for a perceptive mobile network using joint communication and radar sensing," *IEEE Trans. Aerosp. Electron. Syst.*, vol. 56, no. 3, pp. 1926–1941, Jun. 2020.
[33] J. A. Zhang, X. Huang, Y. J. Guo, J. Yuan, and R. W. Heath, "Multibeam for joint communication and radar sensing using steerable analog antenna arrays," *IEEE Trans. Veh. Technol.*, vol. 68, no. 1, pp. 671–685, Jan. 2019.
[34] X. Fu, A. Pedross-Engel, D. Arnitz, C. M. Watts, A. Sharma, and M. S. Reynolds, "Simultaneous imaging, sensor tag localization, and backscatter uplink via synthetic aperture radar," *IEEE Trans. Microw. Theory Techn.*, vol. 66, no. 3, pp. 1570–1578, Mar. 2018.
[35] J. Wang, X.-D. Liang, L.-Y. Chen, L.-N. Wang, and K. Li, "First demonstration of joint wireless communication and high-resolution SAR imaging using airborne MIMO radar system," *IEEE Trans. Geosci. Remote Sens.*, vol. 57, no. 9, pp. 6619–6632, Sep. 2019.
[36] T. Zhang and X.-G. Xia, "OFDM synthetic aperture radar imaging with sufficient cyclic prefix," *IEEE Trans. Geosci. Remote Sens.*, vol. 53, no. 1, pp. 394–404, Jan. 2015.
[37] G. Jin, Y. Deng, W. Wang, Y. Zhang, D. Liang, and R. Wang, "A novel spaceborne MIMO-SAR imaging scheme based on improved OFDM waveforms," *IEEE Geosci. Remote Sens. Lett.*, vol. 18, no. 12, pp. 2122–2126, Dec. 2021.
[38] D. Garmatyuk, J. Schuerger, and K. Kauffman, "Multifunctional software-defined radar sensor and data communication system," *IEEE Sensors J.*, vol. 11, no. 1, pp. 99–106, Jan. 2011.
[39] J. Yang, Y. Tan, X. Yu, G. Cui, and D. Zhang, "Waveform design for watermark framework based DFRC system with application on joint SAR imaging and communication," *IEEE Trans. Geosci. Remote Sens.*, vol. 61, 2023, Art. no. 5200214.
[40] Y. Tan, Z. Li, J. Yang, X. Yu, H. An, J. Wu, and J. Yang, "Joint communication and SAR waveform design method via time-frequency spectrum shaping," *IEEE Trans. Geosci. Remote Sens.*, vol. 60, 2022, Art. no. 5241313.
[41] S. Hu, X. Yuan, W. Ni, and X. Wang, "Trajectory planning of cellular-connected UAV for communication-assisted radar sensing," *IEEE Trans. Commun.*, vol. 70, no. 9, pp. 6385–6396, Sep. 2022.
[42] Z. Zhang, Y. Qu, Z. Wu, M. J. Nowak, J. Ellinger, and M. C. Wicks, "RF steganography via LFM chirp radar signals," *IEEE Trans. Aerosp. Electron. Syst.*, vol. 54, no. 3, pp. 1221–1236, Jun. 2018.
[43] M. Soumekh, *Synthetic Aperture Radar Signal Processing With MATLAB Algorithms*. Hoboken, NJ, USA: Wiley, Apr. 1999.
[44] C. Cafforio, C. Prati, and F. Rocca, "SAR data focusing using seismic migration techniques," *IEEE Trans. Aerosp. Electron. Syst.*, vol. 27, no. 2, pp. 194–207, Mar. 1991.
[45] *Copernicus Data Space Ecosystem*. Accessed: Dec. 13, 2024. [Online]. Available: https://dataspace.copernicus.eu
[46] *Sentinel-1 Mission*. Accessed: Dec. 13, 2024. [Online]. Available: https://sentiwiki.copernicus.eu/web/s1-mission
[47] *sentinel1_level0: Decoding Sentinel1 Level-0 Raw Data*. Accessed: Dec. 13, 2024. [Online]. Available: https://github.com/jmfriedt/sentinel1_level0

ALEX PICCIONI (Member, IEEE) received the master's degree (Hons.) in telecommunications engineering and the Ph.D. degree in information engineering and computer science from the Department of Information Engineering and Computer Science and Mathematics, University of L'Aquila, where he is currently an Assistant Professor. He is a member of the National Inter-University Consortium for Telecommunications (CNIT), Italy. His research activities are focused on mobile network connectivity for urban air mobility systems and software defined radio development for spectral monitoring, integrated sensing and communications, and information embedding techniques.

ROBERTO ALESII (Member, IEEE) received the Laurea and Ph.D. degrees in electronic engineer from the University of L'Aquila, Italy, in 2002 and 2007, respectively. His Ph.D. thesis titled "Communication Protocol Design for Short-Medium Range Systems and Wireless Sensor Networks Design Methodologies Development." He collaborated (since 2002) and he worked (2008–2024) as a degree technical personal with the Centre of Excellence DEWS, University of L'Aquila. He is currently an Assistant Professor. In 2004, he was a co-founder and a member of the Board of Governors of the spin-off company WEST Aquila s.r.l. In 2002, he was a Tutor of the thesis of a certain number of students of both bachelor's and master's degrees. Since 2015, he has been teaching the "Laboratory of SDR, SDN, and the IoT" course with the Department of Information Engineering, Computer Science and Mathematics, University of L'Aquila. Also, he was the Project Manager of some WEST Aquila s.r.l., software defined radio, wireless system embedded and smart water monitoring projects, and he has a contract by the Center of Excellence DEWS for RFiD tag design with WSN integration. He is a member of the National Inter-University Consortium for Telecommunications (CNIT), Italy. He is the author of papers published in various conference proceedings and he has been a reviewer for various international journals. His current research interests mainly focused on wireless communications, mainly for the IoT, with an emphasis on wireless sensor networks, cognitive radio, and software defined radio.

FORTUNATO SANTUCCI (Senior Member, IEEE) received the Laurea and Ph.D. degrees in electronic engineering from the University of L'Aquila, Italy, in 1989 and 1994, respectively. In 1989, he was with Selenia Spazio S.p.a., Rome. From 1991 to 1992, he held a research fellowship with the Solid State Electronics Institute, National Research Council, Rome. Since 1994, he has been with the University of L'Aquila, where he currently holds a position of a Professor of telecommunications with the Department of Information Engineering, Computer Science and Mathematics. He has been a Visiting Researcher with the University of Victoria, Victoria, BC, Canada, and also has been involved in shorter visits with several universities. He is the Principal Investigator of the EMERGE Project on connected vehicles with the University of L'Aquila, is in the board of the Radiolabs Consortium, and in the General Assembly of CNIT. He is a Co-Founder of WEST Aquila s.r.l., a spin-off of the University of L'Aquila. He has held other management positions with the University of L'Aquila, among those he has been a member of the Academic Senate. He is also the Director of the EX-EMERGE Centre of Excellence. He has authored or co-authored over 250 papers in international journals or conference proceedings. His research activity is focused on energy efficient communication paradigms for the Internet of Things, vehicular communication networks, network security, and advanced signal processing for satellite transponders and 5G infrastructures. He has been a member of several technical committees of the IEEE Communications Society. He has served as an Editor for IEEE TRANSACTIONS ON COMMUNICATIONS (2000–2013), *Kluwer Telecommunications Systems*, and other journals.

FABIO GRAZIOSI (Member, IEEE) was born in L'Aquila, Italy, in 1968. He received the Laurea degree (cum laude) and the Ph.D. degree in electronic engineering from the University of L'Aquila, Italy, in 1993 and 1997, respectively. Since February 1997, he has been with the Department of Electrical and Information Engineering, University of L'Aquila, where he currently holds the position of Full Professor in communications systems. The research activity led to more than 200 publications in international journals and conferences and was initially focused on modeling and performance evaluation of wireless systems in complex propagation scenarios. Subsequently, the research approach has been enriched thanks to the contamination with other scientific areas, i.e. electronics, computer science, and control systems. Research activities on wireless sensor networks and networked embedded systems actually fall within this exciting, multidisciplinary context which has been progressively extended to scientific areas historically far from Communications, such as Structural Engineering.

Open Access funding provided by 'CARE-CRUI 2024 Overflow' within the CRUI CARE Agreement